12-2016

Optimization Methodology for CVT Ratio Scheduling with Consideration of Both Engine and CVT Efficiency

Steven Beuerle
Western Michigan University

OPTIMIZATION METHODOLOGY FOR CVT RATIO SCHEDULING WITH CONSIDERATION OF BOTH ENGINE AND CVT EFFICIENCY

by

Steven Beuerle

A thesis submitted to the Graduate College
in partial fulfillment of the requirements
for the degree of Master of Science in Engineering (Mechanical)
Mechanical and Aerospace Engineering
Western Michigan University
December 2016

Thesis Committee:

Jennifer Hudson, Ph. D., Chair
Richard Meyer, Ph. D.
Koorosh Naghshineh, Ph. D.

OPTIMIZATION METHODOLOGY FOR CVT RATIO SCHEDULING WITH CONSIDERATION OF BOTH ENGINE AND CVT EFFICIENCY

Steven Beuerle, M.S.E.

Western Michigan University, 2016

A transmission ratio schedule is developed to optimize the fuel consumption for an automotive continuously variable transmission (CVT) connected to an internal combustion engine (ICE). Although the optimal operating line (OOL) generated from an engine brake specific fuel consumption (BSFC) map can be used to generate a CVT ratio schedule that yields maximum engine efficiency, it was found that OOL-based CVT ratio scheduling does not necessarily offer the best fuel economy because optimal CVT efficiency does not always correspond to OOL tracking. To develop a CVT ratio schedule that can offer the best fuel economy, a novel ratio-scheduling methodology is proposed in this paper. The methodology uses an empirical approach to minimize fuel consumption by considering engine efficiency, CVT efficiency, and requested vehicle power. The proposed CVT ratio scheduling methodology has been simulated using the various portions of the FTP-75 (Federal Test Procedure) cycle. Simulation results show that a significant improvement of engine-CVT overall fuel economy gain is achieved when using the proposed ratio scheduling methodology compared with the case where OOL operation is assumed to yield the highest combined engine-CVT efficiency.

ACKNOWLEDGEMENTS

I would like to thank Dr. Jennifer Hudson of the Mechanical and Aerospace Department at Western Michigan University. This work could not have been possible without her continued guidance and support. I would also like to give a big thank you to Yang Xu, Weitian Chen, Guopeng Hu, Robert Lippert, and Edward Dai, all of the Powertrain Research and Advanced Engineering team at Ford Motor Company, for providing endless support and invaluable knowledge on the topic studied during this thesis. Lastly, I would like to thank Dr. Koorosh Naghshineh and Dr. Richard Meyer for serving on this thesis committee.

Steven Beuerle

TABLE OF CONTENTS

ACKNOWLEDGEMENTS ii

LIST OF TABLES v

LIST OF FIGURES vi

INTRODUCTION 1

Literature Review 4

Assumptions 7

ENGINE EFFICIENCY DATA 7

CVT EFFICIENCY DATA 9

OPTIMIZATION 12

Criteria 12

Methodology 12

Process 15

RESULTS 16

Bag-3 Results Without the CVT Shift Rate Constraint 17

Bag-3 Results With the CVT Shift Rate Constraint 20

CONCLUSIONS AND FUTURE WORK 24

REFERENCES 26

APPENDICES 27

A. Multiple Regression Formulation for CVT Efficiency 27

B. Bag-2 Cycle Results: Without CVT Shift Rate Constraint 32

Table of Contents—Continued

APPENDICES

C. Bag-2 Cycle Results: With CVT Shift Rate Constraint 34

D. Highway Cycle Results: Without CVT Shift Rate Constraint 36

E. Highway Cycle Results: With CVT Shift Rate Constraint 38

LIST OF TABLES

1. Fuel economy results for different portions of the FTP75 cycle 23

LIST OF FIGURES

1. Pulley and belt configuration for a variable diameter CVT 1

2. Sample 4-speed automatic transmission shift schedule 2

3. Sample CVT shift schedule 3

4. Sample speed vs. torque map with derivation of an engine OOL 4

5. Example engine efficiency map after polynomial surface fit and torque weighting 8

6. Regression surfaces for each CVT ratio 11

7. FTP75 cycle with portions highlighted 16

8. Bag-3 optimized speed-torque map: No CVT shift rate constraint 18

9. Bag-3 CVT ratio schedule: No CVT shift rate constraint 18

10. Bag-3 combined powertrain efficiency comparison: No CVT shift rate constraint 19

11. 25-second section of Bag-3 combined powertrain efficiency comparison: No CVT shift rate constraint 19

12. Bag-3 fuel consumption rate comparison: No CVT shift rate constraint 20

13. 25-second section of Bag-3 fuel consumption rate comparison: No CVT shift rate constraint 20

14. Bag-3 optimized speed-torque map: CVT shift rate constraint applied 21

15. Bag-3 CVT ratio schedule: CVT shift rate constraint applied 21

16. Bag-3 combined powertrain efficiency comparison: CVT shift rate constraint applied 22

List of Figures—Continued

17. 25-second section of Bag-3 combined powertrain efficiency comparison:
CVT shift rate constraint applied 22

18. Bag-3 fuel consumption rate comparison:
CVT shift rate constraint applied 23

19. 25-second section of fuel consumption rate comparison:
CVT shift rate constraint applied 23

INTRODUCTION

Improving fuel economy in an automotive powertrain has always been a driving force for continued improvement in the automotive industry. Thus, vehicle powertrain research is constantly searching for ways to change or alter the mechanical operation of a vehicle in order to save fuel. Such research has yielded large advancements in the area of engine power delivery through transmissions. The stepped-ratio gearbox transmission has long been used as the most efficient way to transfer power from the engine to the wheels. However, the continuously variable transmission (CVT) has recently emerged as the more efficient transmission due to the ability of operating within a wide range of gear ratios, coincidentally giving the engine the capability to run near optimum operation for longer periods of time. One type of CVT often used in automotive applications is the variable diameter CVT. This CVT is a belt and pulley system, where the two pulleys are each made of two conical sheaves facing each other. Figure 1 shows a typical configuration of a variable diameter CVT.

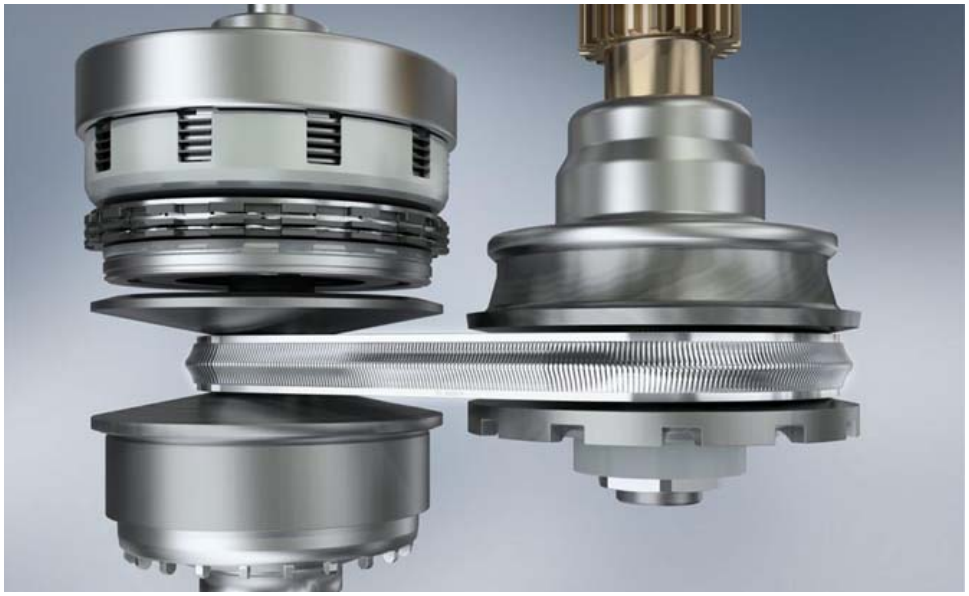

Figure 1: Pulley and belt configuration for a variable diameter CVT [1]

In this type of CVT, the primary pulley is connected to the engine crankshaft, usually separated by a torque converter or centrifugal clutch. The secondary pulley is attached to the driveshaft, and transmits power to the wheels through a final gear reduction. For both pulleys, the sheaves are allowed to move closer and farther apart. Since the width of the belt running between them remains constant, this movement changes the diameter of the pulleys, allowing the speed ratio (hereafter referred to as CVT ratio) between the pulleys to change. This ability allows for the CVT to operate at gear ratios in between the stepped ratios at which the gearbox transmission can explicitly operate, ultimately allowing the engine to consume less fuel for the same power output. Figures 2 and 3 show a sample 4-speed automatic transmission speed map, and a sample CVT speed map, respectively.

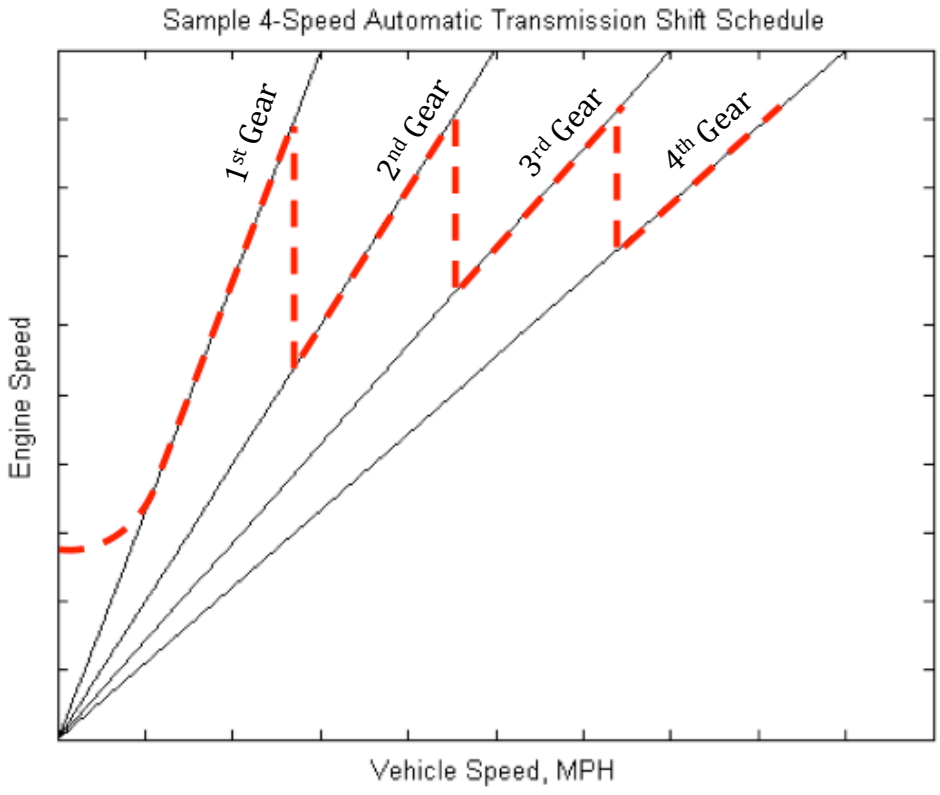

Figure 2: Sample 4-speed automatic transmission shift schedule

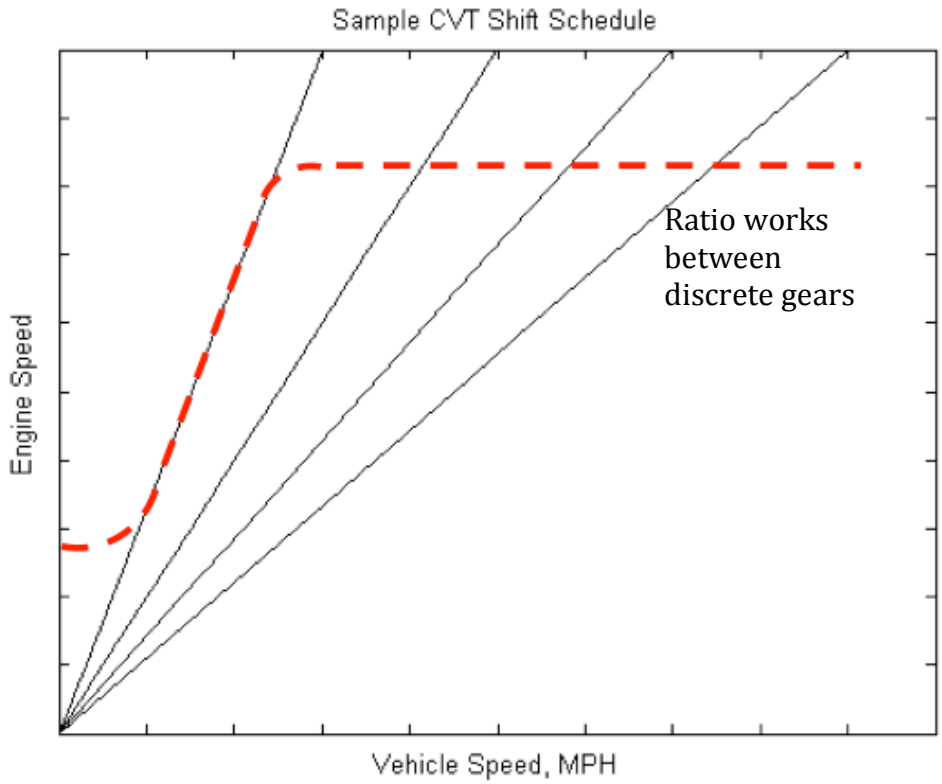

Figure 3: Sample CVT shift schedule

As seen in Figure 2, as the vehicle speed increases, the transmission shifts from gear to gear while simultaneously lowering engine speed. The discrete transmission ratio causes the engine to operate away from the points of optimal engine efficiency. In Figure 3, it is shown that in a CVT, shifting does not occur. Instead the CVT can change ratio as necessary to allow the engine speed to remain constant as the vehicle speeds up. Theoretically, if the engine speed remains closer to the optimal engine operating speed, less fuel is consumed. Due to this fact, there has been a large amount of attention recently towards the study of improving fuel economy by the implementation of CVTs in the automotive driveline.

Both the engine and CVT efficiencies have a direct impact on the fuel economy. It is known that engine efficiency is highest when the engine operates at points along the optimal operating line (OOL). The OOL is defined as the line created by connecting points of least

specific fuel consumption across the operating speed and torque range of the engine. This is shown in Figure 4, where the OOL is constructed by following the gradient of the engine efficiency contour lines.

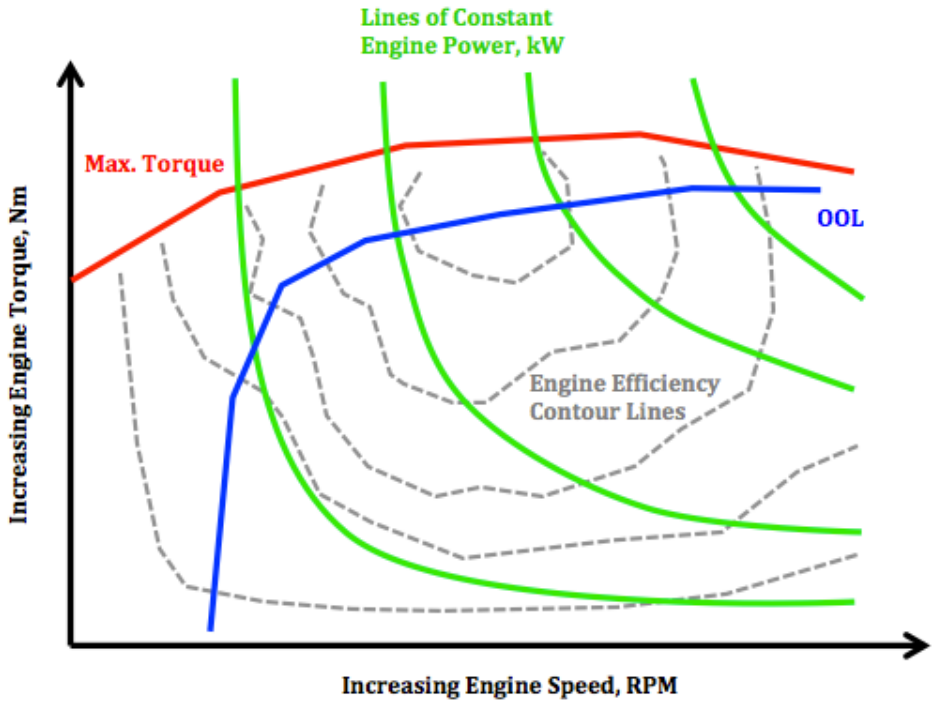

Figure 4: Sample speed vs. torque map with the derivation of an engine OOL.

However, this approach neglects the effects of CVT efficiency. In this paper, we present a CVT ratio scheduling methodology that incorporates varying engine and CVT efficiency while optimizing for lowest fuel consumption based on vehicle power requests.

Literature Review

The foci of previous and current research in this field of study are not always consistent. Therefore, comparison of previous work to the work presented in this paper appears in different areas. Some research has been done with more focus on different methods of control for the

CVT, while other studies have given more attention to the factors that impact the overall powertrain efficiency. First, studies where CVT efficiency is not considered are discussed, followed by those that do consider CVT efficiency. Of the studies where CVT efficiency is considered, other aspects are introduced in order to further separate the presented methodology from previous work.

Bonsen et al. presents a study in which stepped ratio transmissions are compared to CVT-implemented systems [2]. In this study, different ratio control strategies are compared on the basis of fuel economy and drivability measures such as acceleration time. The assumption that using OOL tracking as a method of determining highest efficiency yields the best fuel economy was made in this study, and therefore CVT efficiency was not included. However, we propose that when varying CVT efficiency is considered within the overall efficiency calculation, highest engine efficiency alone does not translate to the best fuel economy. Pfiffner and Guzzella (2003) also assume OOL tracking to be the best way to operate the engine [3]. However, since this study is focused on fuel-optimal control strategies of a CVT during transient operation, the CVT efficiency is assumed to be 100 %, presumably to save time and complexity of the project scope.

Investigating studies that consider CVT efficiency, an earlier study by Pfiffner and Guzzella (2001) focuses only on the optimal operation of CVTs (not the control of them), and presents how the CVT efficiency is modeled when it is not neglected or assumed constant [4]. The observation that CVT efficiency is a three-dimensional function is made, and therefore, a three-dimensional map is developed for the purposes of optimization. This representation of CVT efficiency is comparable to the methodology we present, and results in a more accurate model from an overall powertrain efficiency standpoint. The primary discrepancy between the methodology used in [4] and the proposed methodology in this paper lies within the formulation

of the optimization cost function. In two other studies performed by Ryu and Kim, and Luo et al., CVT efficiency is considered through the use of analytical equations [5,6]. In the methodology presented in this paper, engine and CVT efficiencies, as well as fuel consumption data, are approximated and/or interpolated from empirical data sets. The methods for approximating the data were developed for faster and smoother optimization, thereby reducing computational load and processing time. These methods are discussed in further detail in Chapters 2 and 3 of this paper.

Lastly, a study performed by Lee et al. focuses on control algorithm development with consideration of CVT powertrain response lag time [7]. Within this study, the powertrain lag is cited as a result from a number of factors including CVT shift dynamics, and CVT filling time – the time it takes for the hydraulic fluid to engage the clutches that move the sheaves of the CVT pulleys. Although these factors may contribute to powertrain lag, and therefore a decrease in potential fuel economy, this study does not consider the selection of operation points to improve the CVT efficiency itself. Regardless, this study remains relevant for comparison to the presented work because of the very similar velocity-based approach taken within the optimization of the control algorithm developed in [7].

One last measure divides this work from previous studies: due to the empirical nature of the project, the proposed methodology works in a backwards fashion, using vehicle velocity to determine the wheel power demanded. CVT efficiency is assumed to be the sole contributor in the relationship between demanded wheel power and requested engine power. Fuel power, as a function of engine efficiency, is then optimized subject to the requested power constraint such that the engine power requested is equal to or greater than that which is demanded by the wheels.

This formulation allows the engine to operate away from the OOL when a higher CVT efficiency is achievable within the power and ratio constraints.

Assumptions

Some assumptions of the theoretical system were made to limit the focus of this methodology as well. Torque converter losses are not considered for optimization. Although the torque converter is a vital component for power transferal within the vehicle powertrain, this assumption allows for a simplified optimization problem with fewer constraints. The fluid dynamics and mechanical losses of the torque converter are complex enough that the accuracy gained from including them within the system compared to the added time and width of project focus was not justified. A second assumption made was steady state operating conditions with constant engine coolant and transmission fluid temperature. In reality, it is known that engine and CVT efficiencies are dependent on these operating temperatures. Fluctuation in temperature was neglected for this project.

ENGINE EFFICIENCY DATA

A 2.5L, 4-cylinder internal combustion engine (ICE) was used for this data collection. The engine efficiency was measured at many different engine speed and crankshaft torque values, testing points within the ranges of 600 – 6500 RPM and 20 – 260 Nm, respectively. When plotted, the data create an engine brake specific fuel consumption map. As mentioned in Chapter 1, this map is what determines the shape of the OOL. However, the data set had multiple areas of concern regarding optimization, mainly areas of local maxima. In order to attain a

working surface that would not yield problems within the optimization routine, the empirical data was smoothed in MATLAB using a nonlinear regression surface polynomial fit. The order of this polynomial surface was 4^{th} order in both the engine speed and engine torque dimensions. Although this surface fitting eliminated the areas of local maxima, it was determined that this polynomial surface fit had filtered out too much of the reality of the data. Therefore, a combination of the initial data set and the filtered surface was developed using a torque-weighted relaxation. This alteration eliminated local maxima in the original dataset, while retaining realistic characteristics. A three-dimensional representation of the final map used is shown in Figure 5 where areas of red and blue indicate high and low engine efficiency, respectively.

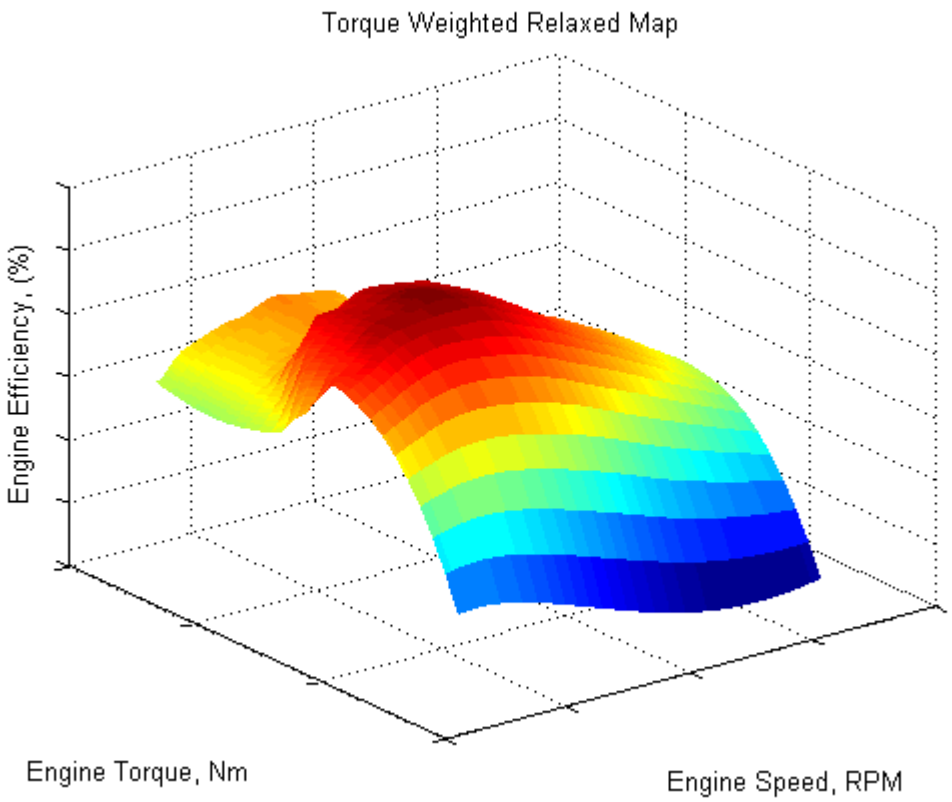

Figure 5: Example engine efficiency map after polynomial surface fit and torque weighting.

Note: Axis values have deliberately been removed to protect the sponsor's sensitive data.

CVT EFFICIENCY DATA

CVT efficiency was determined using benchmarked CVT torque-loss (Nm) data. The CVT efficiency is dependent on three variables: torque converter turbine speed, CVT input torque, and CVT ratio. Torque-loss quantities were measured across ranges of torque converter (TQC) turbine speeds and CVT input torque values. Additionally, this set of measurements was taken at five different CVT ratios. The ranges of TQC turbine speeds and CVT input torque values for this set of measurements were 0 – 6000 RPM and 0 – 250 Nm, respectively. The five CVT ratios at which these measurements were taken were 0.378, 0.7, 1.05, 1.5, and 2.631. Due to the higher dimension set of input variables, a different method for approximating CVT efficiency was needed to create a function that was compatible with the computational optimization.

Multiple linear regression was used to fit the data to a three-dimensional function for the approximation of CVT efficiency at any point. Using the data set available and the known dynamic relationships between the components of the torque converter and the CVT, the predictors for the equation to be developed to determine CVT efficiency can be formulated as functions of three variables: torque input to the CVT, the TQC turbine speed, and the CVT ratio. The regression then gives the coefficients that are combined with these predictors, resulting in a nonlinear function that can approximate the CVT efficiency at any point. This nonlinear function is of the form:

$$\eta_{CVT} = b_1 + \frac{b_2}{\mathrm{T}_{eng}} + b_3\omega_{eng} + b_4 \log r_{CVT} + b_5 \frac{\omega_{eng}}{\mathrm{T}_{eng}} + b_6\omega_{eng} \log r_{CVT} + b_7 \frac{\log r_{CVT}}{\mathrm{T}_{eng}}$$

This form shows that η_{CVT} is a function of the engine speed, engine torque, and the log of the CVT ratio. The b_i values are constant terms found from the output of the regression fitting. This way, the regression only needs to be performed once for the data set, and then this nonlinear function can predict the value of η_{CVT} for any given point between the limits of the benchmark data set. This methodology was derived for this system by Yang Xu of Ford Motor Company and can be found in detail in Appendix A. Figure 6 shows regression surfaces generated using this methodology for each of the five CVT ratios, where areas of red and blue again indicate high and low CVT efficiency.

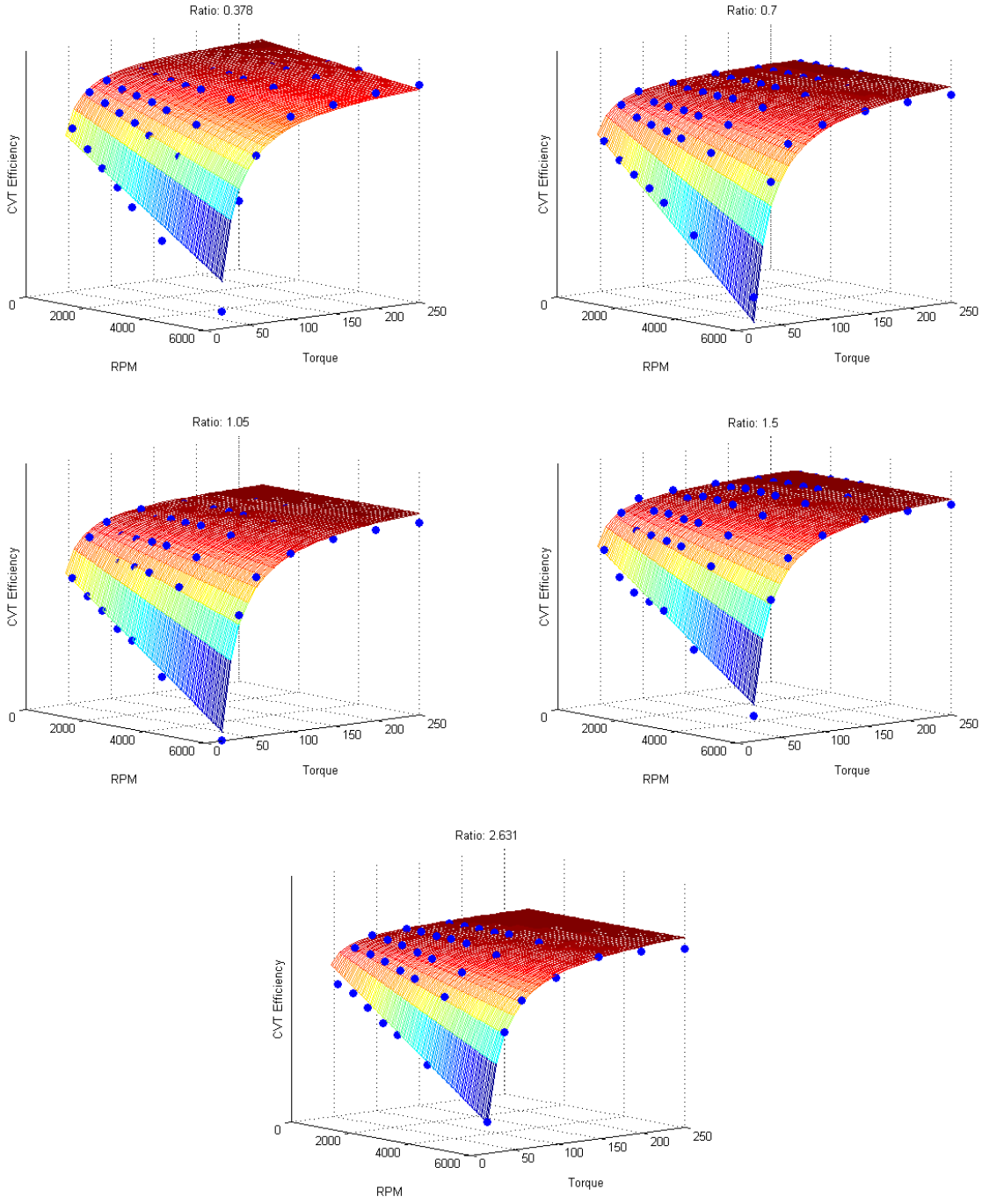

Figure 6: Regression surfaces for each CVT ratio.

Note: Axis values have deliberately been removed to protect the sponsor's sensitive data.

OPTIMIZATION

Criteria

The optimization methodology was developed to optimize combined engine and CVT efficiency during power-on operation. From a vehicle cycle standpoint, this translates to only optimizing during positive acceleration. It is important to note that when the optimization is not being run, CVT efficiency is still being considered in the overall powertrain efficiency. Furthermore, simple limits for locked and unlocked TQC cases were set to govern the optimization routine. When either the engine speed or the forward vehicle speed is below the limit, the TQC is assumed to be slipping, or unlocked, and therefore the optimization is not carried out because of lack of TQC efficiency consideration. The points that do not meet the criteria for optimization as outlined above correspond to points where only engine efficiency is considered.

Methodology

For the case of a locked TQC, (1) primary CVT pulley speed is equal to the engine crankshaft speed, and (2) CVT torque input is equal to engine crankshaft torque output:

$$\omega_{pri} = \omega_{eng} \quad \text{[Eq. 1]}$$

$$\mathrm{T}_{CVT_{in}} = \mathrm{T}_{eng} \quad \text{[Eq. 2]}$$

The methodology is initiated with a given forward vehicle velocity and demanded acceleration. From these parameters, the wheel power needed to meet the acceleration requirement is calculated using dynamic relationships, starting with the calculation of vehicle acceleration,

$$a = \frac{d}{dt}(v), \quad \text{[Eq. 3]}$$

where v is forward vehicle velocity. The force applied to the wheels is then,

$$F_a = ma \quad \text{[Eq. 4]}$$

where m is the vehicle mass. The resistances of rolling friction, air, and grade make up the rest of the forces acting on the vehicle, and are shown in Equations 5 through 8:

$$R_{rolling} = 0.02mg\cos\theta \quad \text{[Eq. 5]}$$

$$R_{air} = 0.5\rho_{air}C_dAv^2 \quad \text{[Eq. 6]}$$

$$R_{grade} = mg\sin\theta \quad \text{[Eq. 7]}$$

$$F_r = R_{rolling} + R_{air} + R_{grade} \quad \text{[Eq. 8]}$$

where g is the acceleration due to gravity, θ is the grade of the driving surface, ρ_{air} is the density of air, C_d is a drag coefficient, and A is the frontal area of the vehicle. Equation 9 then gives the wheel power required to accelerate the vehicle,

$$P_{wheel,demand} = (F_a + F_r) \cdot v \quad \text{[Eq. 9]}$$

From demanded wheel power, the engine power requested is found using CVT efficiency, as shown by Equation 10:

$$P_{eng,request} = \frac{P_{wheel,demand}}{\eta_{CVT}} \quad \text{[Eq. 10]}$$

Equation 10 is one of the constraints used for optimization. Two more constraints come from restricting the CVT ratio between a maximum and minimum predefined ratio:

$$r_{min} \leq r \quad \text{[Eq. 11]}$$

$$r \leq r_{max} \quad \text{[Eq. 12]}$$

The final constraint is a CVT shift rate limit. Since test data was not given for CVT shift speed, the development of this constraint is based on previous work. Pfiffner and Guzzella

(2003) stated that the CVT used in their study could shift from maximum to minimum ratio in roughly two seconds [3]. The maximum ratio difference for that CVT was 5.5. This translates to the CVT shifting through half of the ratio range, 2.75, in about one second. The maximum ratio difference for the CVT used in the work presented was 2.253. This was considered close enough to the half difference observed in [3], so an assumption was made that the CVT used in this work could shift from maximum ratio to minimum ratio in one second. For the case of a time step of 0.1 seconds (as used in the optimization routine), the most the ratio could change by would be 10 percent of the previous value, as shown in Equations 13 and 14.

$$r_{CVT_i} \leq r_{CVT_{i-1}} + \frac{r_{max} - r_{min}}{10} \quad \text{[Eq. 13]}$$

$$r_{CVT_{i-1}} - \frac{r_{max} - r_{min}}{10} \leq r_{CVT_i} \quad \text{[Eq. 14]}$$

Bonsen et al. made mention of shifting being limited to 0.5 Hz for smoothness [2]. Given that the Hertz unit represents cycles per second, the cycle in this case was interpreted as a maximum ratio change. Therefore, the 0.5 Hertz can also be stated as half of a cycle per second (or a full cycle in two seconds), further reinforcing the assumption made in our work, as it is similar to that of [3].

Finally, the objective function to be optimized is an equation that relates fuel power to engine power through the engine speed and engine torque.

$$P_{fuel} = \frac{\omega_{eng} \cdot \mathrm{T}_{eng}}{\eta_{eng}} \quad \text{[Eq.15]}$$

By optimizing fuel power, theoretically, minimal fuel should be consumed while maintaining sufficient engine power to meet the constraint given in Equation 10.

Process

The proposed methodology is an iterative process. In short, velocity and acceleration determine the requested engine power, and therefore, the engine speed and torque. As such, all iterations begin the same way, assuring consistency. The criterion for optimization then determines how each iteration is carried out. As described in Chapter 1, the optimization is only applied in the power-on case, and locked torque converter condition. In cases that don't meet the criterion, some constraints are still placed on the OOL tracking in order to remain within the realm of drivability. For instance, under circumstances that do not meet the criteria for optimization, ratio limits and shift rate limits are still enacted on the system even though CVT efficiency is not being considered. This assures realistic CVT operation throughout the full schedule.

Further steps were taken to guarantee accuracy in the results. As detailed in the previous sections, the data for engine and CVT efficiencies was modified slightly to present more optimization-friendly functions. However, it is important to note that empirically gathered data is not always accurate. Therefore, the alteration of inaccurate data could theoretically lead to inaccurate approximations. In optimization, inaccurate approximations can lead to local maxima within the data, where an optimized solution may converge. To eliminate this possibility of local maximum convergence, a further iteration procedure was developed for the optimization routine. Starting with the engine operation point that coincides with the power requested by the engine, many random seed points were generated within a defined space around this starting point. Each seed point is then optimized, and the point(s) that consume the least fuel is taken as the optimal solution.

RESULTS

MATLAB was used to test the proposed methodology. The Bag-3, Bag-2, and Highway portions of the FTP75 cycle were used as the cycle velocity input, and change in fuel economy was used as the sole comparator. Figure 7 shows the entire FTP75 cycle.

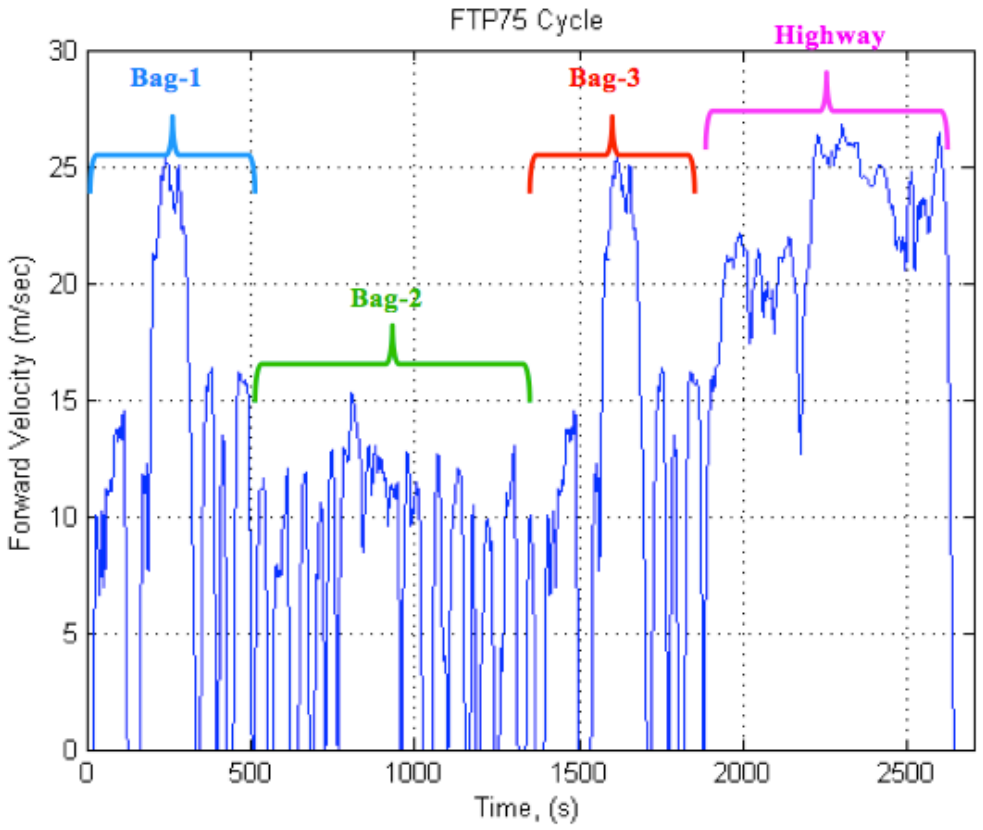

Figure 7: FTP75 cycle with portions highlighted.

Notice in Figure 7 that the Bag-1 and Bag-3 portions are identical. The difference between these two portions is that Bag-1 is a cold start, meaning the engine has not warmed up to operating temperature. Recall that this affects the powertrain efficiency, and we have neglected this change in temperature for this study. Bag-3 presents the same cycle portion, but a steady state operating temperature is assumed.

Results for the Bag-3, Bag-2, and Highway portions of the FTP75 cycle have been obtained for two scenarios: one where the CVT shift rate constraint has not been applied, and one where it has been. This was done to illustrate how the addition of a CVT shift rate constraint alters the resulting CVT ratio schedule. Therefore, we first present the results that correspond to the scenario lacking the shift rate constraint, followed by the results where the shift rate has been included. Furthermore, the results for both scenarios for all portions of the FTP75 cycle display very similar characteristics, thus only the Bag-3 results are discussed in detail below. Percent change in fuel economy for each cycle is also presented. The results for both scenarios for the Bag-2 and Highway cycles can be found in Appendices A, B, C, and D.

Bag-3 Cycle Results Without the CVT Shift Rate Constraint

To start analyzing the results, the first plot investigated is Figure 8, where the optimized solutions (red), and the un-optimized solutions (cyan) are plotted point by point on the engine speed versus engine torque plane. The original OOL is shown as a solid blue line for reference. The corresponding ratio schedule for this set of results is shown in Figure 9.

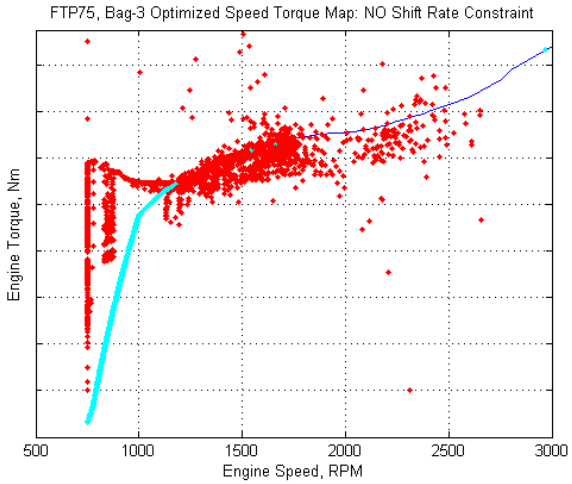

Figure 8: Bag-3 optimized speed-torque map: No CVT shift rate constraint.

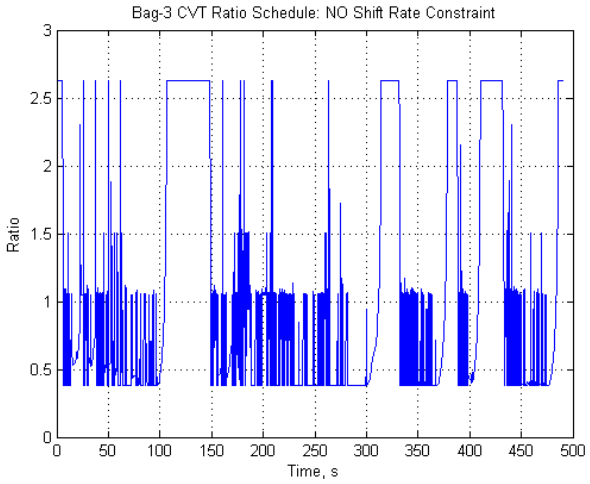

Figure 9: Bag-3 CVT ratio schedule: No CVT shift rate constraint.

Note: Axis values have deliberately been removed to protect the sponsor's sensitive data.

Two interesting characteristics are noticed when analyzing this plot. First, starting around 1200 RPM and moving left, many optimized solutions seem to deviate away from the OOL towards a region of high torque and low engine speed. This phenomenon is due to low acceleration (and therefore low wheel power demand), and trends observed in the CVT efficiency contours. As seen in Figure 6, areas of high torque and low engine speed exhibit higher CVT efficiency, thus the optimal solutions tend to deviate in that direction when the power request is not a limiting factor. Similarly, the vertical line of red solutions located near an engine speed of roughly 750 RPM indicate those solutions that met the criteria for optimization, but observed a very low power request, and therefore deviated towards the highest CVT efficiency before meeting the engine idle speed constraint. In these situations, CVT efficiency played the dominant role in the overall powertrain efficiency calculation. The second characteristic of interest is in the region of 1800-2500 RPM. The majority of optimal solutions in this region fall below the original OOL. This is believed to occur because in that region, the

change in CVT efficiency is not enough to justify deviating away from an area of higher engine efficiency.

Figure 10 displays the combined powertrain efficiency for the Bag-3 cycle without a CVT shift rate constraint, while Figure 11 shows a zoomed section of the same plot as to illustrate better how the optimization routine is working. This section exhibits characteristics that are present throughout the entire cycle.

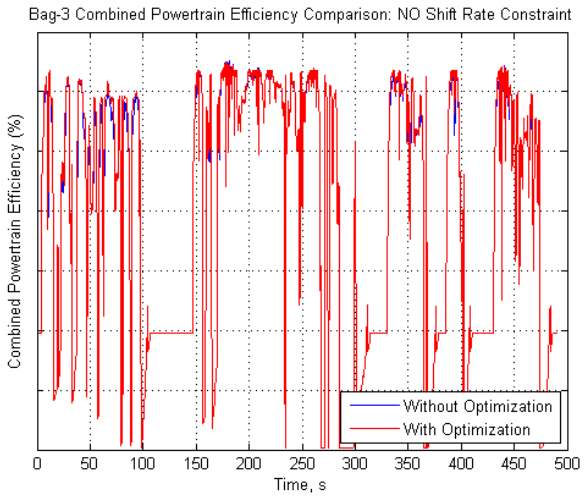

Figure 10: Bag-3 combined powertrain efficiency comparison: No CVT shift rate constraint.

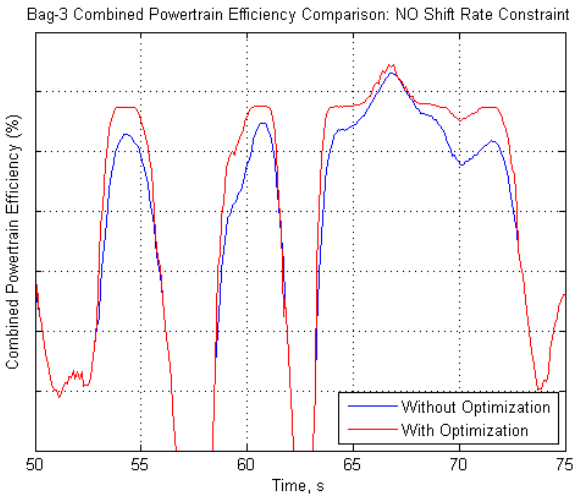

Figure 11: 25-second section of Bag-3 combined powertrain efficiency comparison: No CVT shift rate constraint.

Note: Axis values have deliberately been removed to protect the sponsor's sensitive data.

The portions of Figure 11 where the two curves overlap correspond to solutions where the optimization is not being run, and OOL tracking is being performed. These solutions therefore remain on the OOL, as represented in Figure 8 by the un-optimized points. In other sections of the plot, the optimized solutions often result in higher overall combined powertrain efficiency than the un-optimized solutions. This confirms that the optimization problem

formulation is correct and the routine is working as expected. Figures 12 and 13 compare the fuel consumption rate without a CVT shift rate constraint in a similar manner.

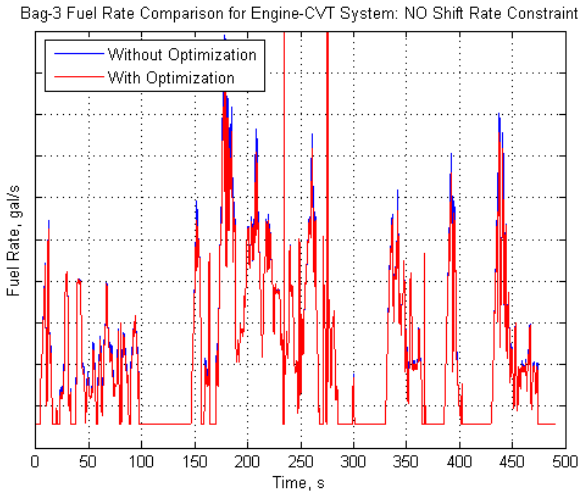

Figure 12: Bag-3 fuel consumption rate comparison: no CVT shift rate constraint.

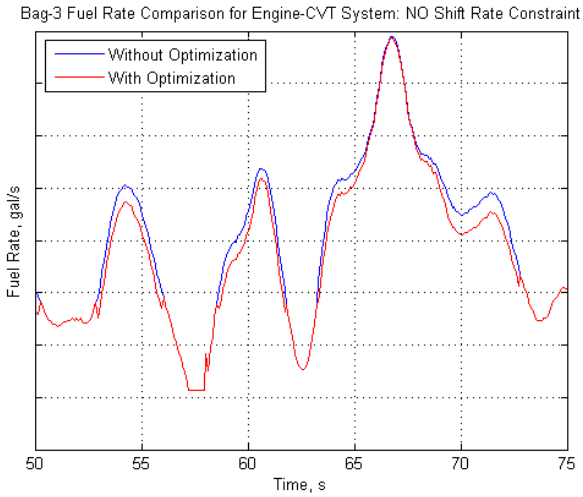

Figure 13: 25-second section of Bag-3 fuel consumption rate comparison: no CVT shift rate constraint.

Note: Axis values have deliberately been removed to protect the sponsor's sensitive data.

The same trend from Figure 11 is also present in Figure 13, where the optimal points yield a lower fuel consumption rate than those that follow the OOL. Again, this 25-second section depicts characteristics seen throughout the entire cycle shown in Figure 12. The increase in combined powertrain efficiency results in a decrease in fuel consumption, thereby leading to an increase in fuel economy for the Bag-3 cycle.

Bag-3 Cycle Results With the CVT Shift Rate Constraint

As observed in Figure 9, there were many points during the Bag-3 cycle where the CVT ratio would instantaneously jump to a minimum or maximum value. These points correspond to the abnormal solutions seen in Figure 8. Although these spikes in ratio are caused by solutions

that mathematically meet all constraints on the system, this does not represent a realistic shift schedule because the CVT cannot operate that quickly. The addition of a CVT shift rate constraint as formulated in Chapter 4, limits the shifting to a percentage of the maximum ratio difference, and therefore eliminates these spikes in the CVT ratio schedule. The results for the scenario where the CVT shift rate has been applied show a much cleaner optimized speed-torque map, and CVT ratio schedule, as shown in Figures 14 and 15, respectively. However, it is important to note that this comes at the sacrifice of a portion of the improvement in fuel economy observed.

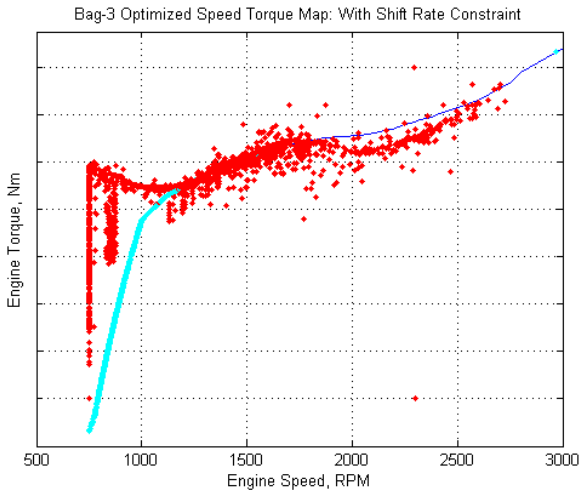

Figure 14: Bag-3 optimized speed-torque map: CVT shift rate constraint applied.

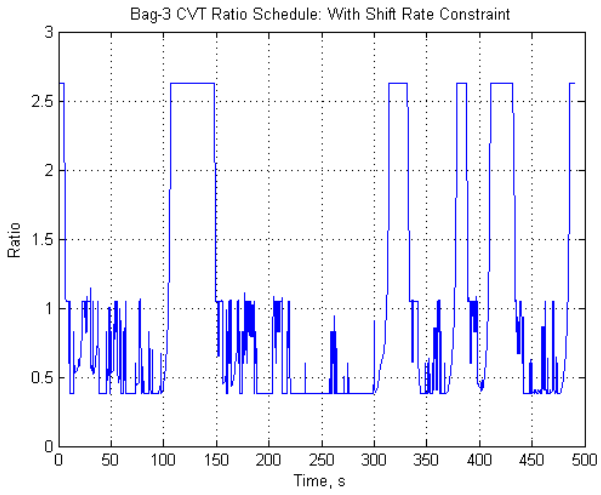

Figure 15: Bag-3 CVT ratio schedule: CVT shift rate constraint applied.

Note: Axis values have deliberately been removed to protect the sponsor's sensitive data.

With the addition of the CVT shift rate constraint, the optimized combined powertrain efficiency curve changes very slightly. When the CVT ratio change is limited from one point to the next, the optimal solution may yield a slightly smaller combined powertrain efficiency compared to the case where it was not limited. Figures 16 and 17 show the combined powertrain

efficiency comparison again, and small differences can be seen between the shift-limited solution in Figure 17, and the solution from Figure 11.

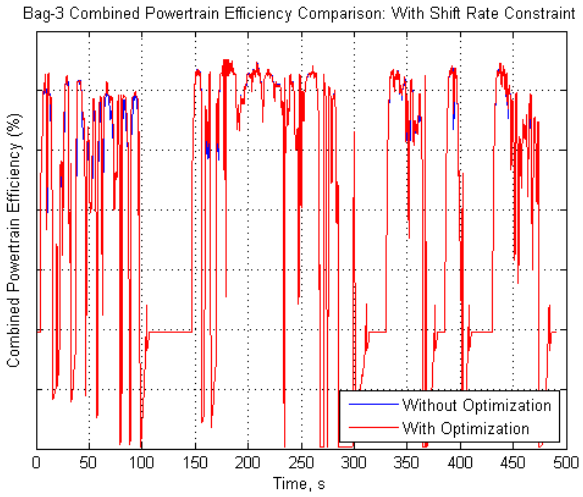

Figure 16: Bag-3 combined powertrain efficiency comparison: CVT shift rate constraint applied.

Figure 17: 25-second section of Bag-3 combined powertrain efficiency comparison: CVT shift rate constraint applied.

Note: Axis values have deliberately been removed to protect the sponsor's sensitive data.

The same trend is also seen in the fuel consumption rate comparison plots in Figure 18 and 19. Again, the CVT shift rate constraint limits the solution at some points. Very similar to the comparison between Figures 17 and 11 for the optimized combined powertrain efficiency curves, small differences can be seen between the optimized fuel consumption rate curves in Figures 19 and 13.

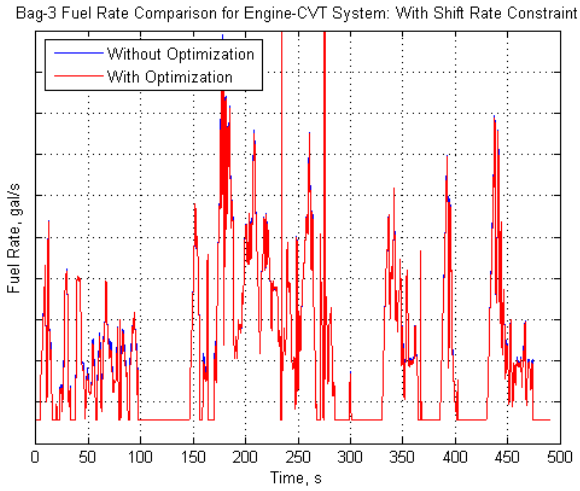

Figure 18: Bag-3 fuel consumption rate comparison: CVT shift rate constraint applied.

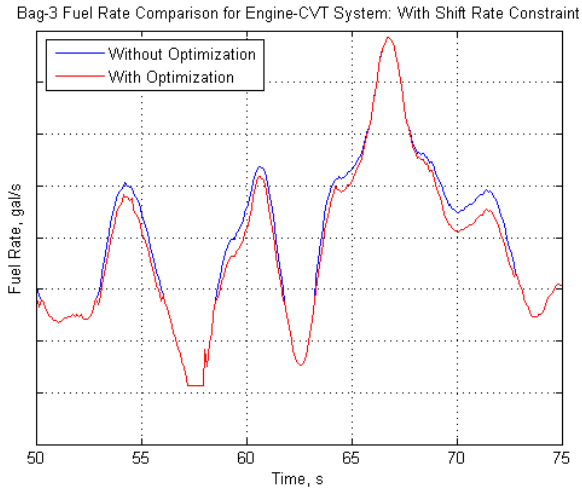

Figure 19: 25-second section of Bag-3 fuel consumption rate comparison: CVT shift rate constraint applied.

Note: Axis values have deliberately been removed to protect the sponsor's sensitive data.

These small changes between the two scenarios yield slightly different overall fuel economy changes between the optimized and un-optimized solutions. The percent increase in fuel economy for both scenarios of all three portions of the FTP75 cycle are displayed in Table 1.

Table 1: Fuel economy results for different portions of the FTP75 cycle

FTP75 Cycle Portion	% Change Without Shift Rate Constraint	% Change With Shift Rate Constraint
Bag-3	+ 2.9222 %	+ 1.2808 %
Bag-2	+ 3.4561 %	+ 2.5566 %
Highway	+1.2354 %	+ 0.2621 %

As expected, for all three sections of the FTP75 cycle, in the scenarios where the CVT shift rate is not constrained, the percent change in fuel economy is larger than in those for which the shift rate constraint has been applied. Another observation is that the highway results show a

smaller percent increase than those seen for the Bag-3 and Bag-2 results. This is expected because of the nature of highway driving. Not as much variation in vehicle speed (and therefore engine speed) over time indicates that the optimization would not be needed as frequently as the Bag-3 and Bag-2 cycles. Regardless, each portion of the cycle resulted in an increase in fuel economy when the optimization was allowed, and therefore validates the methodology.

CONCLUSIONS AND FUTURE WORK

The methodology presented in this paper has been compared to previous work in a comprehensive literature review. Measures have been taken to assure the scope of this project presents something new in the field of CVT ratio scheduling. Once developed, the methodology was then modeled and simulated in MATLAB using three separate FTP75 cycle inputs. Each input results in an increase in fuel economy, implying a successful optimization routine was developed. To maintain realistic operation, a CVT shift rate constraint was then added to the system. These results were compared with the results found prior to the addition of this constraint. It was shown that even with the new constraint, positive changes in fuel economy were still observed, although the magnitude of percent change in fuel economy was slightly smaller. It is evident that with this methodology, lower fuel consumption rates can be obtained when the engine operating point is allowed to deviate from the OOL if a higher CVT efficiency is attainable. This shows the importance in accounting for a varying CVT efficiency, and optimizing fuel power such that the overall engine-CVT efficiency is increased. Therefore, we suggest that neglecting the effects of CVT efficiency and assuming OOL tracking to be the optimal approach results in the sacrifice of fuel economy.

Finally, it is important to note that the proposed ratio scheduling methodology only results in a target CVT ratio schedule. As such, future work can focus on the control theory development and implementation to further improve fuel economy or drivability of the system using this ratio scheduling methodology to develop a target schedule for which the control theory can be developed.

REFERENCES

[1] Crowe, P., 2013, "Basic CVT Insight," from http://www.hybridcars.com/basic-cvt-insight/

[2] Bonsen, B., Steinbuch, M., and Veenhuizen, P. A., 2005, "CVT ratio control strategy optimization," *2005 IEEE Vehicle Power and Propulsion Conference,* pp. 227-231.

[3] Pfiffner, R., Guzzella, L., Onder, C. H., 2003, "Fuel-optimal control of CVT powertrains," *Control Engineering Practice,* **11**(3), pp. 329-336.

[4] Pfiffner, R., Guzzella, L., 2001, "Optimal Operation of CVT-based Powertrains," *International Journal of Robust and Nonlinear Control,* **11**, pp. 1003-1021.

[5] Ryu, W., and Kim, H., 2008, "CVT Ratio Control with Consideration of CVT System Loss," *International Journal of Automotive Technology,* **9**(4), pp. 459-465.

[6] Luo, Y., Sun, D., Qin, D., Chen, R., and Hu, F., 2010, "Fuel optimal control of CVT equipped vehicles with consideration of CVT efficiency," *Journal of Mechanical Engineering,* **46**(4), pp. 80-86.

[7] Lee, H., Kim, C., Kim, T., Kim, H., 2004, "CVT Ratio Control Algorithm by Considering Powertrain Response Lag," *Transmission and Driveline Symposium.*

APPENDIX A

Multiple Regression Formulation for CVT Efficiency

One assumption made for this model is that the relationships between the TQC and the CVT are linear. If the relationships are examined using one variable at a time (i.e. – the other two are held constant), the CVT torque-loss can then be expressed by two equations formulated using two different approaches:

Approach 1: Given a fixed CVT ratio (r_{CVT}) and CVT input torque ($\mathrm{T}_{CVT_{in}}$), the torque loss can be expressed as:

$$\mathrm{T}_{loss} = a + b \cdot \omega_{TQC_{turbine}} \quad \text{[Eq. 16]}$$

where *a* and *b* are functions of the fixed variables:

$$a = f_1(r_{CVT}, \mathrm{T}_{CVT_{in}}) \quad \text{[Eq. 17]}$$

$$b = g_1(r_{CVT}, \mathrm{T}_{CVT_{in}}) \quad \text{[Eq. 18]}$$

Approach 2: Given a fixed CVT ratio (r_{CVT}) and TQC turbine speed, ($\omega_{TQC_{turbine}}$), the torque loss can be expressed as:

$$\mathrm{T}_{loss} = c + d \cdot \mathrm{T}_{CVT_{in}} \quad \text{[Eq. 19]}$$

where *c* and *d* are functions of the fixed variables:

$$c = f_2(r_{CVT}, \omega_{TQC_{turbine}}) \quad \text{[Eq. 20]}$$

$$d = g_2(r_{CVT}, \omega_{TQC_{turbine}}) \quad \text{[Eq. 21]}$$

If the input torque to the CVT is small, or if the rotational speed of the TQC turbine is small, losses are still contributed to the system through Equations 17 and 20. Equations 18 and 21 represent the slope between the change in CVT torque loss and the change in input torque, and the slope between the change in CVT torque loss and the change in TQC turbine speed, respectively.

In order to translate the torque loss data to CVT efficiency, Equation 22 is used:

$$\eta_{CVT} = \frac{\mathrm{T}_{CVT_{in}} - \mathrm{T}_{loss}}{\mathrm{T}_{CVT_{in}}} \quad \text{[Eq. 22]}$$

If Equations 16 and 19 are substituted into Equation 22, CVT efficiency is then expressed in terms of CVT torque input and TQC turbine speed. First, by substituting Equation 16, we arrive at Equation 23:

$$\eta_{CVT} = \frac{\mathrm{T}_{CVT_{in}} - (a + b \cdot \omega_{TQC_{turbine}})}{\mathrm{T}_{CVT_{in}}} \quad \text{[Eq. 23]}$$

After some rearrangement of Equation 23, Equation 24 becomes:

$$\eta_{CVT} = \frac{T_{CVT_{in}} - a}{T_{CVT_{in}}} - \frac{b}{T_{CVT_{in}}} \cdot \omega_{TQC_{turbine}} \quad \text{[Eq. 24]}$$

Recall that for this case, CVT input torque is held constant. Therefore, simplifying the constant terms gives Equations 25 and 16:

$$A = \frac{T_{CVT_{in}} - a}{T_{CVT_{in}}} \quad \text{[Eq. 25]}$$

$$B = -\frac{b}{T_{CVT_{in}}} \quad \text{[Eq. 26]}$$

Substitute Equations 25 and 26 into Equation 24 to get a simplified form in Equation 27:

$$\eta_{CVT} = A + B \cdot \omega_{TQC_{turbine}} \quad \text{[Eq. 27]}$$

The form of Equation 27 implies that the CVT efficiency can be predicted by a linear equation with a nonzero constant. Therefore, the first two regression predictors are:

$$P_1 = 1\ (constant) \quad \text{[Eq. 28]}$$

$$P_2 = \omega_{TQC_{turbine}} \quad \text{[Eq. 29]}$$

Using the same substitution method, but with Equation 19, we get:

$$\eta_{CVT} = \frac{\mathrm{T}_{CVT_{in}} - (c + d \cdot \mathrm{T}_{CVT_{in}})}{\mathrm{T}_{CVT_{in}}} \quad \text{[Eq. 30]}$$

Again after some rearranging of terms:

$$\eta_{CVT} = (1 - d) - \frac{c}{\mathrm{T}_{CVT_{in}}} \quad \text{[Eq. 31]}$$

Simplifying the constant terms from Equations 20 and 21 gives Equation 32 and 33:

$$C = -c \quad \text{[Eq. 32]}$$

$$D = 1 - d \quad \text{[Eq. 33]}$$

Substituting Equations 32 and 33 into Equation 31 gives a simplified form in Equation 34:

$$\eta_{CVT} = D + \frac{C}{\mathrm{T}_{CVT_{in}}} \quad \text{[Eq. 34]}$$

Again, Equation 34 is a linear equation with a nonzero constant term. So the third regression predictor is:

$$P_3 = \frac{1}{\mathrm{T}_{CVT_{in}}} \quad \text{[Eq. 35]}$$

A fourth predictor can be developed by analysis of varying CVT ratio when TQC turbine speed and CVT torque input are held constant. In this case, torque-loss was approximated as a logarithmic relationship to the CVT ratio. Therefore, the fourth predictor is:

$$P_4 = \log(r_{CVT}) \quad \text{[Eq. 36]}$$

After initial analysis, it was speculated that it is not sufficient to look at these variables one at a time. Often, they vary together, so the interactions of the four variables together give us three more predictors. By combining Equations 28, 29, 35 and 36 together through multiplication, we get Equations 37 through 39:

$$P_5 = \frac{\omega_{TQC_{turbine}}}{\mathrm{T}_{CVT_{in}}} \quad \text{[Eq. 37]}$$

$$P_6 = \omega_{TQC_{turbine}} \cdot \log(r_{CVT}) \quad \text{[Eq. 38]}$$

$$P_7 = \frac{\log(r_{CVT})}{\mathrm{T}_{CVT_{in}}} \quad \text{[Eq. 39]}$$

Recall that the focus of this problem formulation is for a locked torque converter. This introduces two major assumptions:

1. Torque converter turbine speed is equal to the engine crankshaft speed:

$$\omega_{TQC_{turbine}} = \omega_{eng} \quad \text{[Eq. 40]}$$

2. Torque applied to the CVT is equal to the torque being transferred by the crankshaft:

$$\mathrm{T}_{CVT_{in}} = \mathrm{T}_{eng} \quad \text{[Eq. 41]}$$

Substituting Equations 40 and 41 into the equations derived for each predictor yields a slightly different set of equations for the predictors of the data. Notice that Equations 28 and 36 did not change after these assumptions were applied. All seven predictors are now given as:

$$P_1 = 1\ (constant) \quad \text{(no change) [Eq. 28]}$$

$$P_2 = \omega_{eng} \quad \text{[Eq. 42]}$$

$$P_3 = \frac{1}{\mathrm{T}_{eng}} \quad \text{[Eq. 43]}$$

$$P_4 = \log(r_{CVT})$$ (no change) [Eq. 36]

$$P_5 = \frac{\omega_{eng}}{\mathrm{T}_{eng}}$$ [Eq. 44]

$$P_6 = \omega_{eng} \cdot \log(r_{CVT})$$ [Eq. 45]

$$P_7 = \frac{\log(r_{CVT})}{\mathrm{T}_{eng}}$$ [Eq. 46]

An *n*-by-*p* matrix of predictors to fit to the *p* predictors at each of the *n* observations is then constructed by the predictors that were chosen. Matrix *P* is shown as:

$$[P] = \begin{bmatrix} 1 & \frac{1}{\mathrm{T}_{eng}(1)} & \omega_{eng}(1) & \log r_{CVT}(1) & \frac{\omega_{eng}(1)}{\mathrm{T}_{eng}(1)} & \omega_{eng}(1) \cdot \log r_{CVT}(1) & \frac{\log r_{CVT}(1)}{\mathrm{T}_{eng}(1)} \\ 1 & \frac{1}{\mathrm{T}_{eng}(2)} & \omega_{eng}(2) & \log r_{CVT}(2) & \frac{\omega_{eng}(2)}{\mathrm{T}_{eng}(2)} & \omega_{eng}(2) \cdot \log r_{CVT}(2) & \frac{\log r_{CVT}(2)}{\mathrm{T}_{eng}(2)} \\ \vdots & \vdots & \vdots & \vdots & \vdots & \vdots & \vdots \\ 1 & \frac{1}{\mathrm{T}_{eng}(n)} & \omega_{eng}(n) & \log r_{CVT}(n) & \frac{\omega_{eng}(n)}{\mathrm{T}_{eng}(n)} & \omega_{eng}(n) \cdot \log r_{CVT}(n) & \frac{\log r_{CVT}(n)}{\mathrm{T}_{eng}(n)} \end{bmatrix}$$

The regression fitting outputs a *p*-by-1 vector *b* of predictor coefficients. These coefficients are then applied to the predicting equation such that any point in the data surface can be approximated. The result is Equation 47.

$$\eta_{CVT} = b_1 + \frac{b_2}{\mathrm{T}_{eng}} + b_3\omega_{eng} + b_4 \log r_{CVT} + b_5 \frac{\omega_{eng}}{\mathrm{T}_{eng}} + b_6\omega_{eng} \log r_{CVT} + b_7 \frac{\log r_{CVT}}{\mathrm{T}_{eng}}$$ [Eq. 47]

APPENDIX B

Bag-2 Cycle Results: Without CVT Shift Rate Constraint

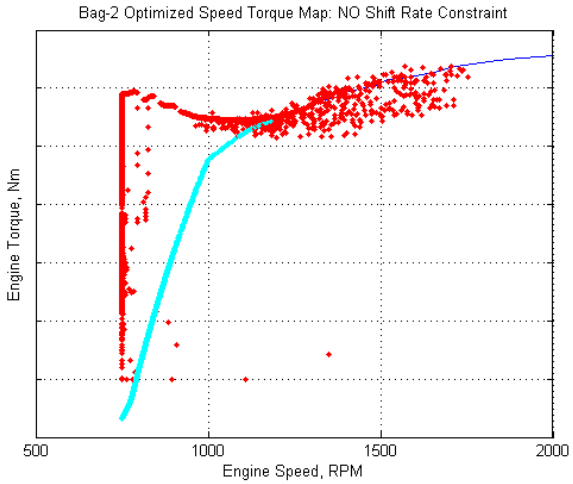

Figure 20: Bag-2 optimized speed-torque map: No CVT shift rate constraint.

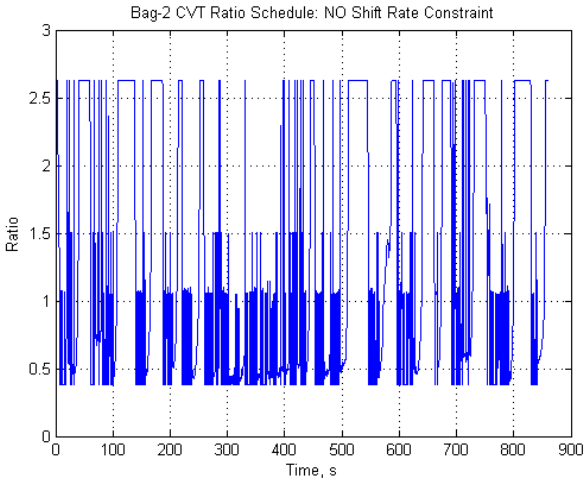

Figure 21: Bag-2 CVT ratio schedule: No CVT shift rate constraint.

Note: Axis values have deliberately been removed to protect the sponsor's sensitive data.

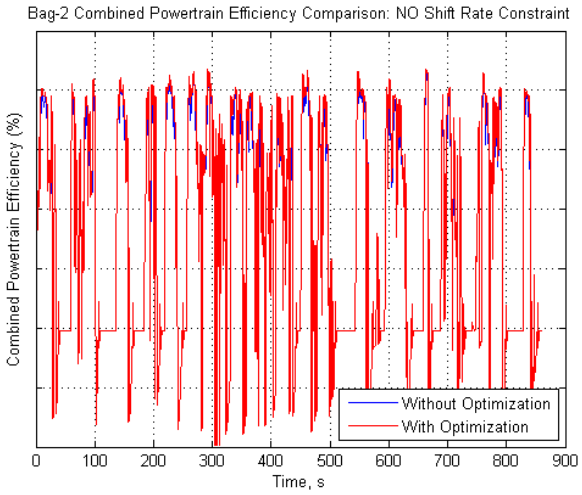

Figure 22: Bag-2 combined powertrain efficiency comparison: No CVT shift rate constraint.

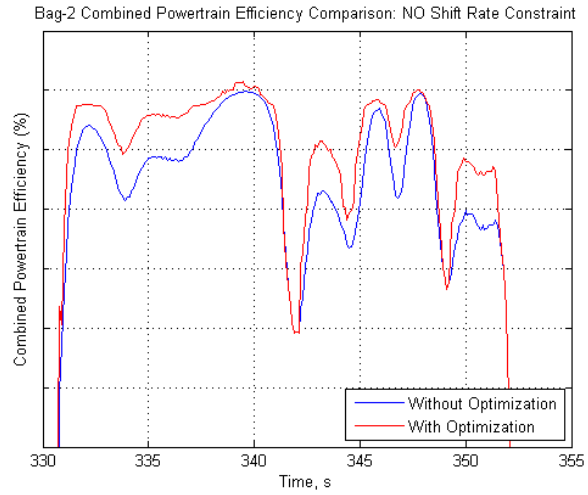

Figure 23: 25-second section of Bag-2 combined powertrain efficiency comparison: No CVT shift rate constraint.

Note: Axis values have deliberately been removed to protect the sponsor's sensitive data.

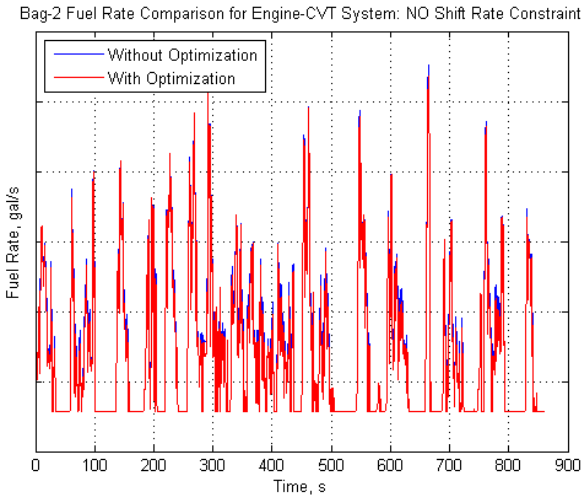

Figure 24: Bag-2 fuel consumption rate comparison: No CVT shift rate constraint.

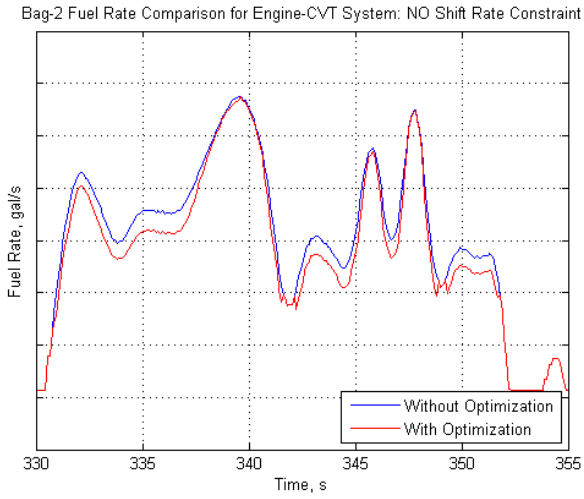

Figure 25: 25-second section of Bag-2 fuel consumption rate comparison: No CVT shift rate constraint.

Note: Axis values have deliberately been removed to protect the sponsor's sensitive data.

APPENDIX C

Bag-2 Cycle Results: With CVT Shift Rate Constraint

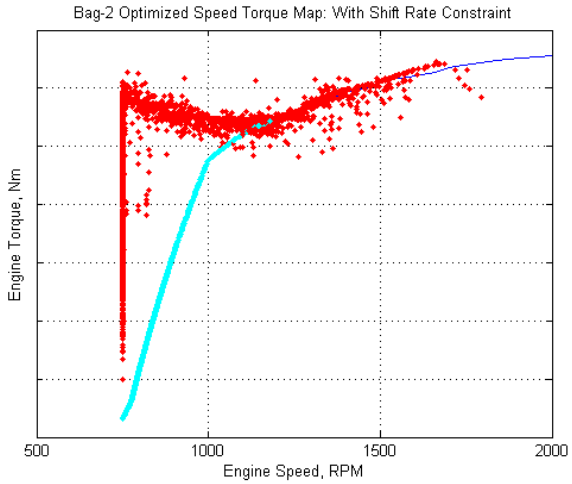

Figure 26: Bag-2 optimized speed-torque map: CVT shift rate constraint applied.

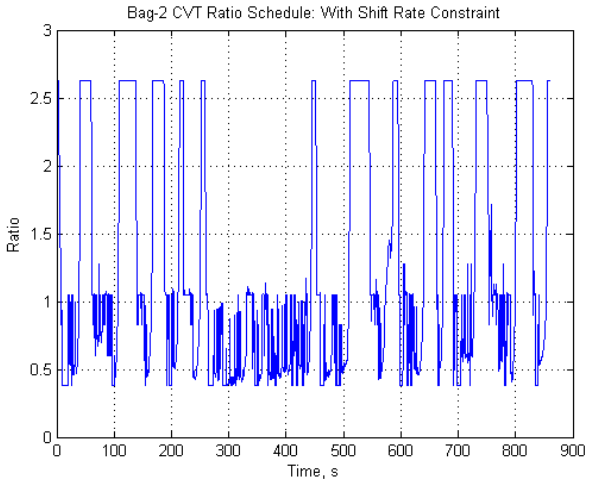

Figure 27: Bag-2 CVT ratio schedule: CVT shift rate constraint applied.

Note: Axis values have deliberately been removed to protect the sponsor's sensitive data.

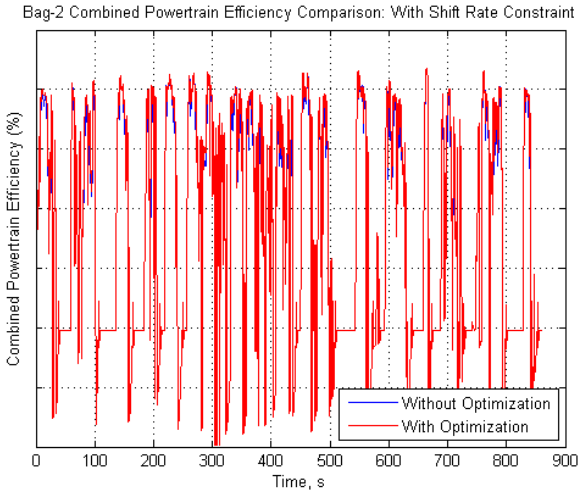

Figure 28: Bag-2 combined powertrain efficiency comparison: CVT shift rate constraint applied.

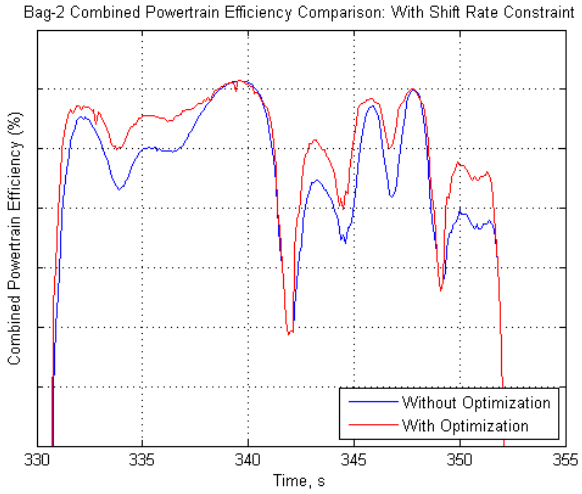

Figure 29: 25-second section of Bag-2 combined powertrain efficiency comparison: CVT shift rate constraint applied.

Note: Axis values have deliberately been removed to protect the sponsor's sensitive data.

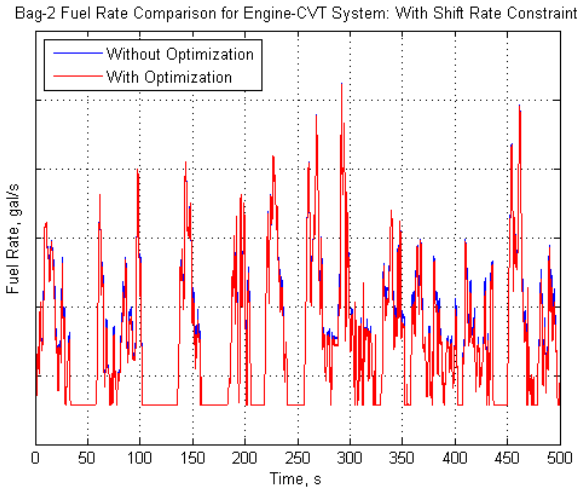

Figure 30: Bag-2 fuel consumption rate comparison: CVT shift rate constraint applied.

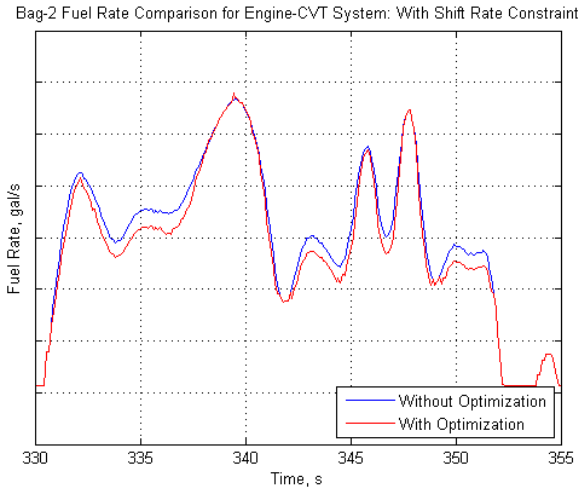

Figure 31: 25-second section of Bag-2 fuel consumption rate comparison: CVT shift rate constraint applied.

Note: Axis values have deliberately been removed to protect the sponsor's sensitive data.

APPENDIX D

Highway Cycle Results: Without CVT Shift Rate Constraint

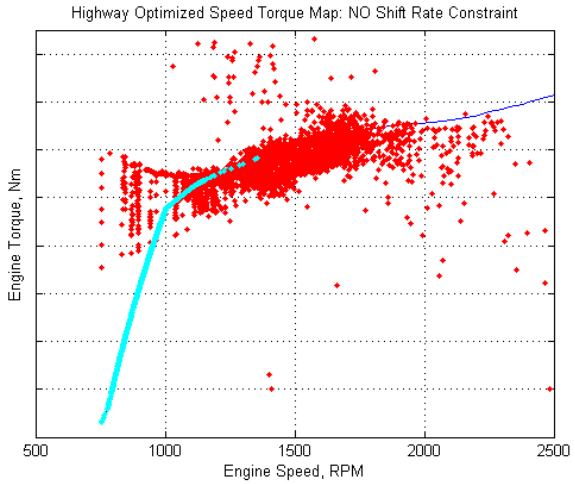

Figure 32: Highway optimized speed-torque map: No CVT shift rate constraint.

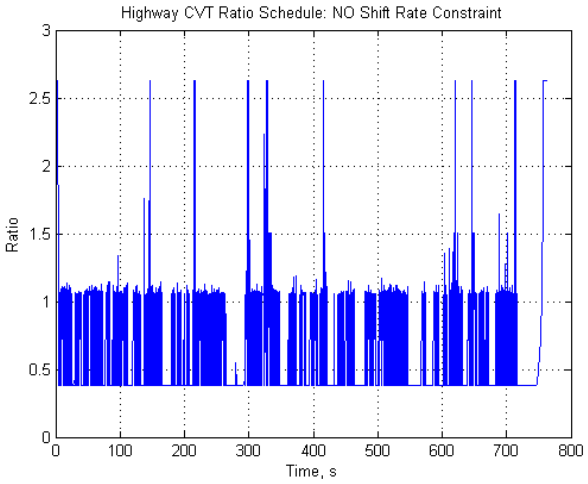

Figure 33: Highway CVT ratio schedule: No CVT shift rate constraint.

Note: Axis values have deliberately been removed to protect the sponsor's sensitive data.

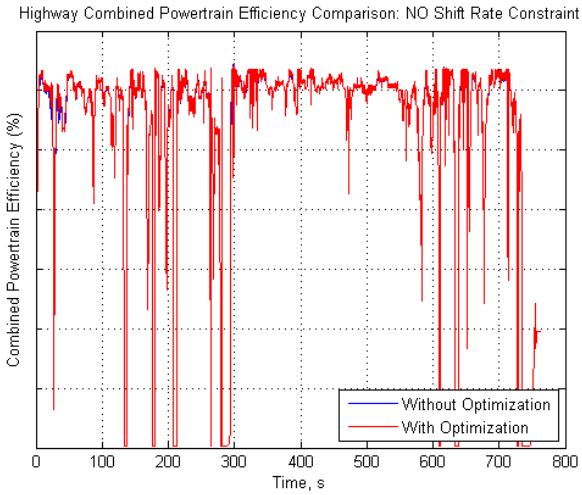

Figure 34: Highway combined powertrain efficiency comparison: No CVT shift rate constraint.

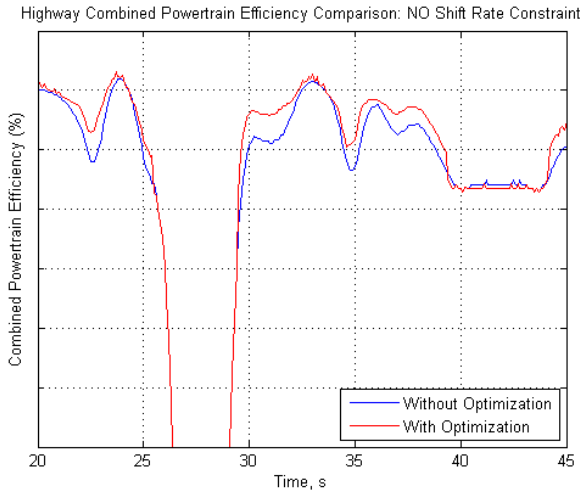

Figure 35: 25-second section of Highway combined powertrain efficiency comparison: No CVT shift rate constraint.

Note: Axis values have deliberately been removed to protect the sponsor's sensitive data.

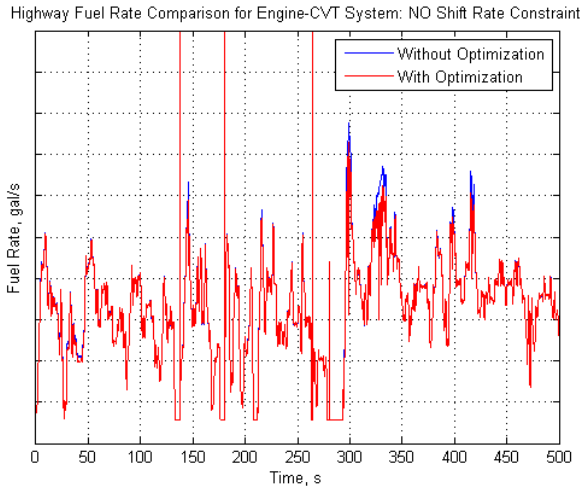

Figure 36: Highway fuel consumption rate comparison: No CVT shift rate constraint.

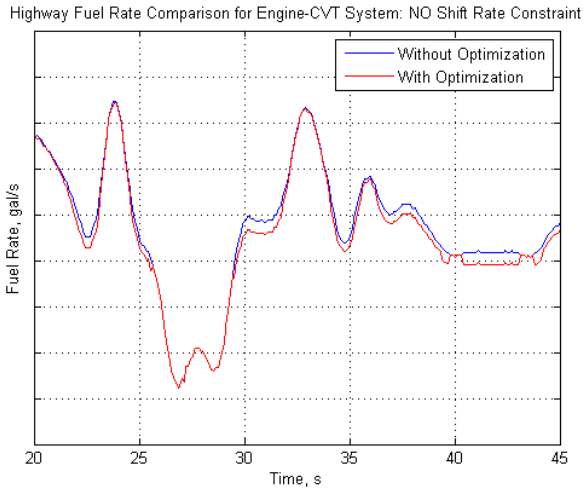

Figure 37: 25-second section of Highway fuel consumption rate comparison: No CVT shift rate constraint.

Note: Axis values have deliberately been removed to protect the sponsor's sensitive data.

APPENDIX E

Highway Cycle Results: With CVT Shift Rate Constraint

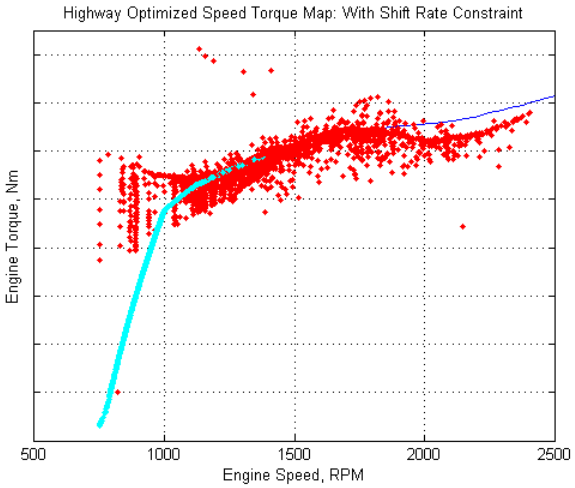

Figure 38: Highway optimized speed-torque map: CVT shift rate constraint applied.

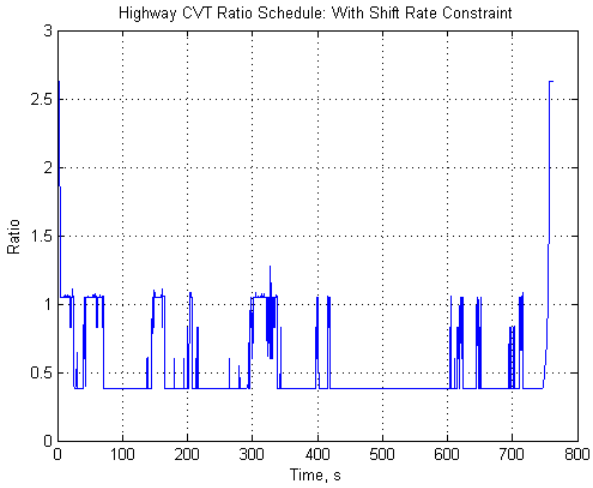

Figure 39: Highway CVT ratio schedule: CVT shift rate constraint applied.

Note: Axis values have deliberately been removed to protect the sponsor's sensitive data.

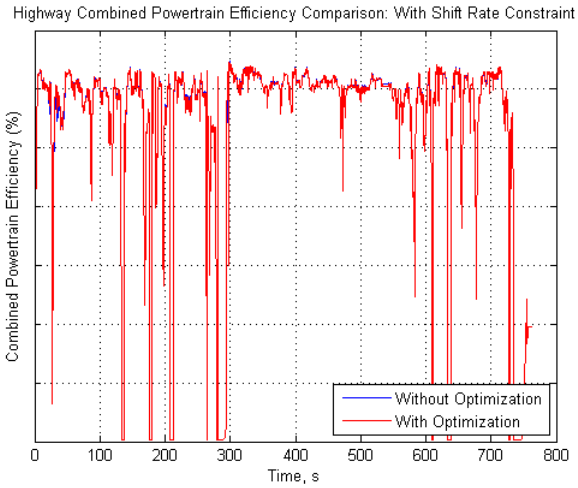

Figure 40: Highway combined powertrain efficiency comparison: CVT shift rate constraint applied.

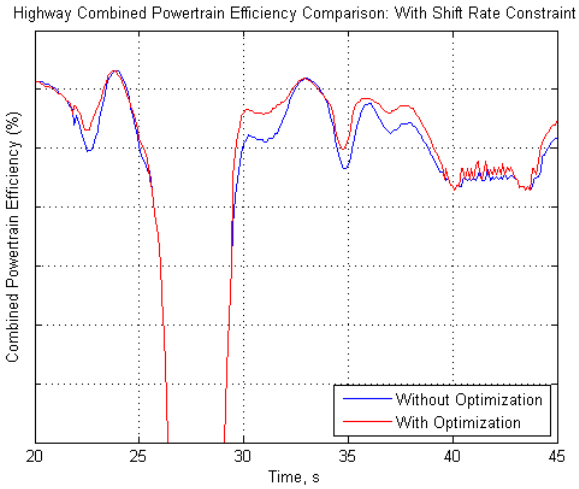

Figure 41: 25-second section of Highway combined powertrain efficiency comparison: CVT shift rate constraint applied.

Note: Axis values have deliberately been removed to protect the sponsor's sensitive data.

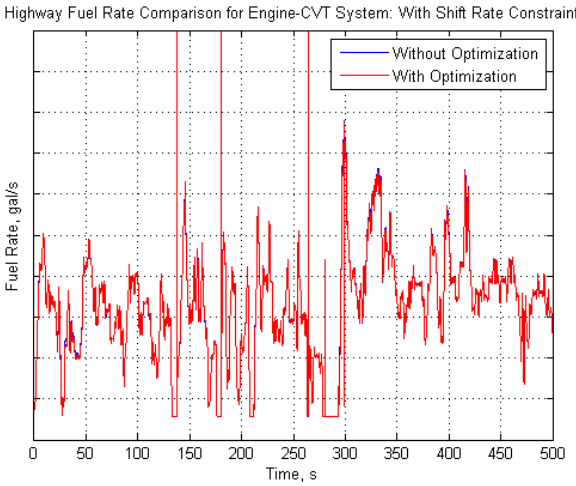

Figure 42: Highway fuel consumption rate comparison: CVT shift rate constraint applied.

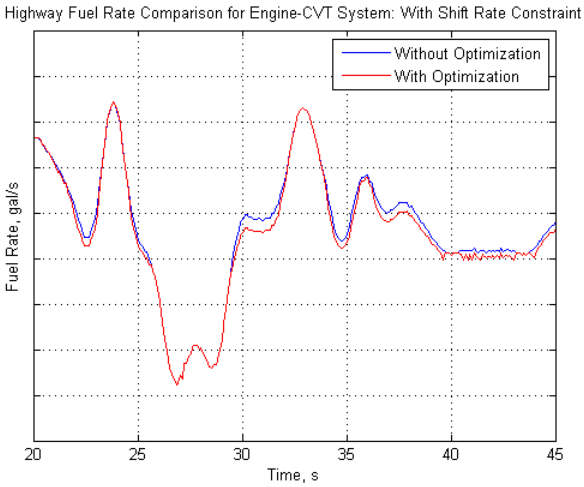

Figure 43: 25-second section of Highway fuel consumption rate comparison: CVT shift rate constraint applied.

Note: Axis values have deliberately been removed to protect the sponsor's sensitive data.